A computer-aided temporal and dynamic subtraction technique of the liver for detection of small hepatocellular carcinomas on abdominal CT images

メタデータ	言語: eng
	出版者:
	公開日: 2017-10-03
	キーワード (Ja):
	キーワード (En):
	作成者:
	メールアドレス:
	所属:
URL	http://hdl.handle.net/2297/2927

1   Title of article:

2   Computer-aided temporal and dynamic subtraction technique of the liver for detection of small

3   hepatocellular carcinoma on abdominal CT images

4

5   Authors and Addresses:

6   E Okumura[1], S Sanada[1], M Suzuki[1] and O Matsui[2]

7

8   1. Department of Radiological Technology Graduate School of Medical Sciences Kanazawa

9   University

10   5-11-80 Kodatsuno, Kanazawa, 920-0942, Japan

11   2. Department of Radiology, Kanazawa University School of Medicine

12   Kanazawa, Japan

13

14   Short Title:

15   Computer-aided temporal and dynamic subtraction technique of the liver for detection of small

16   HCC on abdominal CT images

17

21

22   ABSTRACT:

23   It is often difficult for radiologists to identify small hepatocellular carcinoma (HCC) due to

24   insufficient contrast enhancement. Therefore, we have developed a new computer-aided

25   temporal and dynamic subtraction technique to enhance small HCC, after automatically

26   selecting images set at the same anatomical position from the present (non-enhanced and

27   arterial-phase CT images) and previous images. The present study was performed with CT

28   images from fourteen subjects. First, we used template-matching based on similarities in liver

1

1 shape between the present (non-enhanced and arterial-phase CT images) and previous

2 arterial-phase CT images at the same position. Temporal subtraction images were then obtained

3 by subtraction of the previous image from the present image taken at the same position of the

4 liver, and dynamic subtraction images were also obtained by subtraction of non-enhanced CT

5 images from arterial-phase CT images taken at the same position of the liver. Twenty-one of 22

6 nodules (95.5%) with contrast enhancement were visualised in temporal and dynamic

7 subtraction images. Increases of 150% and 140% in nodule-to-liver contrast were observed on

8 dynamic and temporal subtraction images compared with present arterial-phase CT images,

9 respectively. These subtraction images may be useful as reference images in detection of small

10 moderately differentiated HCC.

11

1   1. INTRODUCTION

2   The number of patients with hepatocellular carcinoma (HCC) is increasing worldwide.

3   Therefore, patients in high-risk groups consisting of those with liver cirrhosis and hepatitis B, C

4   undergo routine screening (Farinati and Gianni 2001, Ward and Robinson 2002). Although

5   ultrasonography (US) is widely used in screening for HCC, it has limitations in the detection of

6   small tumours (Kim *et al.* 2001). Therefore, abdominal CT examination is also performed

7   (Ward and Robinson 2002). However, hypervascular tumours are often located adjacent to

8   vascular structures and are often minute. It is especially difficult for radiologists to distinguish

9   true HCC from small nodular arterioportal shunt (A-P shunt) in patients with liver cirrhosis.

10   Therefore, the sensitivity of CT examination for detection of HCC is low, ranging from only

11   59%–68% (Peterson *et al.* 2000, Baron and Peterson 2001, Blachar *et al.* 2002).

12   Hypervascular moderately differentiated HCC usually exhibits early enhancement on

13   arterial-phase CT images and ring enhancement on delayed-phase CT images. However, it is

14   necessary to differentiate HCC from small A-P shunts, because the latter often show nodular

15   enhancement on arterial-phase CT images. Therefore, the development of methods for

16   computer-aided diagnosis (CAD) is required to avoid overlooking nodular early enhancement

17   and to increase the reliability of diagnostic imaging of HCC.

18   A number of groups have reported dynamic subtraction techniques for US, CT and MRI

19   of the liver region (Soyer *et al.* 1999, Hong *et al.* 2001, Spielmann *et al.* 2002, Yu and Rofsky

20   2003). However, use of these techniques in routine clinical practice requires the selection of US,

21   CT and MR images at the same anatomical position, increasing both the time required and cost

22   as radiologists must visually select images at the same positions of the liver. In a preliminary

23   study, we developed an automated image registration technique to allow the selection of image

24   sets corresponding to the same anatomical positions from non-enhanced and arterial-phase CT

25   images (Okumura *et al.* 2005). Using this automated image registration technique, we have

26   developed a new dynamic subtraction technique to detect early enhancement, including

27   moderately differentiated HCC and A-P shunts.

28   A number of groups have also reported temporal subtraction techniques for chest CT

29   images and posteroanterior (PA) chest images (Kano *et al.* 1993, Ishida *et al.* 1998, Ishida *et al.*

1999, Abe *et al.* 2004). These investigators reported that temporal subtraction techniques enhanced many subtle changes in chest CT images and PA chest images. However, to our knowledge, there have been no previous reports regarding the detection of HCC by temporal subtraction. Therefore, we have developed a new temporal subtraction technique to detect increases in size of nodular early enhancement and new enhancement, after automatically selecting images set at the same anatomical positions from present and previous CT images.

2. Materials and methods

2.1 Materials

The study population consisted of fourteen patients with HCC (ten men and four women; mean age, 65.1 years). Pairs of images (previous and present images) were obtained for each patient. Each patient underwent non-enhanced and arterial-phase CT imaging of the upper abdomen using a LightSpeed Utra16 scanner (GE Yokogawa Medical Systems, Tokyo, Japan; 120 kVp and 200 mA). The matrix size of the images was 512×512 pixels, and the slice thickness and number of images in fourteen examinations were 1.25–3.75 mm and 65–200 images, respectively. The previous and present images were obtained from October 2002 to June 2004, and the interval between images was 174±80.5 days (range, 84 to 377 days). Based on prospective interpretation of the present images, radiologists suspected 18 HCCs and 1 A-P shunt, and missed 5 tumours. Based on the previous images, radiologists suspected 6 HCCs and 6 A-P shunts. Twenty-four nodules, including the 5 missed tumours, were diagnosed as HCC on angiography, CT hepatic arteriography (CTHA) and CT arterial portography (CTAP) performed after the present CT examination.

2.2 Development of computer algorithm

The application described here was developed using Borland C++ Builder 6 (Borland, Scotts Valley, CA, USA). The CT images were transferred off-line from a CT scanner to a personal computer (PC) with a 2.0 GHz CPU.

2.3 Detection of the liver region

1   The right hepatic lobe occupies almost the entire right half of the abdomen on CT images,

2   and the shape of the liver region changes gradually in the cranial to caudal direction. However,

3   it is often difficult to extract all liver regions using methods based only on detecting the

4   maximum area, because the left and right lobes may be visualised separately, and the spleen and

5   other organs may have areas larger than the liver in some images.

6   The image centre of gravity in the liver region does not show marked variation in the

7   neighbouring images. We attempted to detect the liver region in all images taking into

8   consideration the centre of gravity in the top and bottom images.

9   The present non-enhanced and arterial-phase CT images and the previous arterial-phase

10   CT images were smoothed. A rectangular region of interest (ROI) was set manually at the centre

11   of the liver region on the reference image, in the middle of the craniocaudal portion of the liver.

12   We obtained the threshold value of the liver in this ROI by histogram analysis and binarised all

13   images using this threshold value. These binary images were obtained where a pixel was

14   assigned a value of 0 or 1 if the density was below or above the threshold value, respectively.

15   We employed opening processing (erosion and dilation) to eliminate the extrahepatic structures,

16   such as the abdominal wall and stomach, and the centre of gravity of the labelled regions was

17   calculated after labelling. The labelled regions of the adjacent images, including the centre of

18   gravity of the image, were then detected as the liver region (Okumura *et al.* 2005).

19

20   *2.4 Image matching of the same anatomical positions*

21   Image matching has been carried out to identity the posteroanterior and lateral views

22   of chest radiographs (Arimura *et al.* 2002) and for patient recognition of previous and current

23   chest radiographs (Morishita *et al.* 2001, Morishita *et al.* 2004) using intensity-based methods,

24   which make use of residual and correlation coefficients, *etc.*

25   The residual, *R*, which indicates the extent of similarity between template *A (i, j)* and

26   training images *B (i, j)*, was determined as follows:

27
$$R = \sum_{j=1}^{M} \sum_{i=1}^{N} | A(i, j) - B(i, j) | \qquad\qquad (1)$$

28   The matrix size for the template and training images was $M \times N$. By comparison of the residual

29   between template and training images, the template images can be considered as training images

1   that provide lesser residuals. In the present study, we used the residual for image-matching of

2   the same anatomical positions, because we produced binarised arterial-phase CT images as

3   template images and binarised non-enhanced CT images as training images, and it was useful to

4   show image subtraction with the sum of intensity differences.

5

6   *2.5 Dynamic subtraction technique*

7   First, we produced binarised present arterial-phase CT images as template images, and

8   binarised non-enhanced CT images as training images. To register the present non-enhanced and

9   arterial-phase CT images obtained in the same period, we used template-matching (automated

10   image-matching) based on similarities in liver shape between the present non-enhanced and

11   arterial-phase CT images at the same position. Automated image-matching was then applied to

12   determine the global shift value ($\Delta x,\ \Delta y$) between the two images showing the best match,

13   which corresponds to the shift in the *x, y* coordinates of the template images relative to the shift

14   in the *x', y'* coordinates of training images (Ishida *et al.* 1998) using Eq.(2):

15      $x' = x + \Delta x$

16      $y' = y + \Delta y$ (2)

17   After performing the global shift ($\Delta x,\ \Delta y$), dynamic subtraction images were

18   obtained by subtraction of non-enhanced CT images from arterial-phase CT images taken at the

19   same position of the liver.

20

21   *2.6 Temporal subtraction technique*

22   First, we produced binarised present arterial-phase CT images as template images, and

23   the binarised previous arterial-phase CT images as training images. Then, we registered the

24   previous and present arterial-phase CT images at the same position in the same manner as

25   described for dynamic subtraction. After performing the global shift ($\Delta x,\ \Delta y$), temporal

26   subtraction images were obtained by subtraction of the previous images from the present

27   images taken at the same position of the liver.

28

29   *2.7 Subjective evaluation of the quality of dynamic and temporal subtraction images*

30   All cases were assessed by three experienced radiologists after consultation with no

knowledge of the presence of HCC in all cases. Four sets of CT images were evaluated for the presence of HCC, and were classified as: (a) presence of HCC, (b) suspected HCC, and (c) no HCC. Set A (only present non-enhanced CT images) was assessed first, followed by set B (present non-enhanced and arterial-phase CT images), set C (non-enhanced, arterial-phase, and previous arterial-phase CT images), and set D (set C plus dynamic and temporal subtraction images), and this cycle was then repeated. In addition, the image quality of dynamic and temporal subtraction images indicating confirmed or suspected HCC in set C was assessed by three radiologists using a three-point score: 3 (good), whole nodule was visualised with minor misregistration; 2 (adequate), nodule was visualised with some misregistration; and 1 (poor), nodule was not detected with marked misregistration error. Finally, the usefulness of both subtraction images in detecting HCC was classified as follows: +1, very helpful; 0, no additional information; and −1, not helpful.

2.8 Objective evaluation of the quality of dynamic and temporal subtraction images

To allow objective evaluation of the quality of dynamic subtraction images using the present CT images and temporal subtraction images, we calculated the nodule-to-liver contrast (Contrast) and signal-to-noise ratio (SNR) of the present arterial-phase CT images and dynamic subtraction images using the present CT images and temporal subtraction images (Biswas *et al.* 2005) according to Eq. (3) and (4):

$$Contrast = CT_{nodule} - CT_{liver} \qquad (3)$$

$$SNR = CT_{nodlue\_or\_liver} / SD_{air} \qquad (4)$$

We selected regions of interest (ROIs) for the liver and the lesion. Five ROIs of about 10 × 10 pixels were deposited manually in the liver region. We measured the average value of five ROIs, which was defined as CT_{liver} of the liver region. The boundary of the nodule was traced manually to measure the ROI for the nodule region. We measured CT_{nodule} in the nodule region in the same manner as described for measurement of CT number in the liver region. We measured the standard deviation (SD_{air}) of the background to estimate image noise. Respective data for Contrast and SNR between the present arterial-phase CT images and temporal subtraction images, and between the present arterial-phase CT images and dynamic subtraction images using the present CT images with good rating score were analysed using Wilcoxon's

1 two-tailed paired *t*-test, and $P \leq 0.05$ was considered statistically significant.

2

3

4 **3. Results**

5   Three experienced radiologists detected 21 of 24 HCCs (87.5%), suspected HCC in one

6 case, and missed 2 HCCs in sets A–C. Twenty-two of 24 HCCs (91.6%) were detected, HCC

7 was suspected in one case, and one HCC was not detected in set D. There were no incidences of

8 false-positives. The temporal and dynamic subtraction images enhanced the detection of HCC.

9 With regard to image quality of dynamic and temporal subtraction images, 21 HCCs were

10 classified as good and one HCC as poor. With regard to the image quality of dynamic

11 subtraction images alone, 20 HCCs showing nodular early enhancement were classified as good,

12 while in the image quality of temporal subtraction image alone, 16 HCCs showing ring or

13 nodular enhancement were classified as good.

14   On subtraction images, none of 7 HCCs with nodular enhancement on the present images

15 showed abnormal enhancement on the previous images. All 7 HCCs showing nodular

16 enhancement on the dynamic subtraction images were classified as good, while 5 of 7 HCCs

17 showing nodular enhancement on the temporal subtraction images were classified as good (Fig.

18 1). Fourteen HCCs suspected to be nodular lesions on the previous images showed increases in

19 size on the present images. Twelve of 14 HCCs showing nodular enhancement on dynamic

20 subtraction images were classified as good, while 10 of 14 HCCs showing ring enhancement on

21 temporal subtraction images were classified as good (Fig. 2). One HCC was suspected based on

22 previous and present images; enhanced lesions were seen on both temporal and dynamic

23 subtraction images in this HCC and the results were classified as good (Fig. 3). With regard to

24 the usefulness of subtraction images, three of 21 HCCs classified as good were classified as

25 very helpful. The subtraction images increased the conspicuousness of detection of HCC (Fig.

26 4).

27   However, one HCC detected in sets A–C was not visualised on both subtraction images

28 (Fig. 5), and was classified as poor.

29   The averages and SD of nodule-to-liver contrast and nodule-to-liver contrast ratio of the

30 present arterial-phase CT images and temporal subtraction images, and dynamic subtraction

images using the present CT images are shown in Table 1. For good rating score of dynamic subtraction images using the present images and temporal subtraction images compared with the present arterial-phase CT images, dynamic subtraction images using the present CT images and temporal subtraction images were 150% and 140% increases in nodule-to-liver contrast, respectively ($P<0.01$). In addition, the averages and SD of SNR and ratio of SNR of the present arterial-phase CT images and temporal subtraction images, and dynamic subtraction images using the present CT images of the liver and nodule region are also shown in Table 1. For good rating score of dynamic subtraction images using the present CT images and temporal subtraction images compared with the present arterial-phase CT images, dynamic subtraction images using the present CT images and temporal subtraction images showed deterioration in SNR, respectively ($P<0.01$). In cases in which both subtraction images were mostly registered with only minor misregistrations, nodule-to-liver contrast of both subtraction images was higher than those of the present arterial-phase CT images, and SNR of both subtraction images was lower than those of the present arterial-phase CT images in the liver and nodule region.

4. Discussion

It is often difficult for radiologists to detect HCC adjacent to vascular structures and to distinguish them from other small hypervascular tumours or small nodular A-P shunts (Peterson *et al.* 2000, Baron and Peterson 2001, Blachar *et al.* 2002). Using the method described here, 21 of 22 nodules (95.5%) showed nodular enhancement and/or ring enhancement on dynamic and temporal subtraction images and were classified as good. Twenty of 22 nodules (90.9%) showed nodular early enhancement on dynamic subtraction images and were classified as good. Sixteen of 22 nodules (72.7%) showed ring enhancement, showing an increase in size or new enhancement on temporal subtraction images and were classified as good. In addition, dynamic subtraction images were useful in assisting in the detection of early enhancement, such as moderately differentiated HCC and A-P shunts. Temporal subtraction images showed an increase of ring enhancement in the lesions in the previous arterial-phase CT images that indicated the presence of HCC and nodular enhancement showed the appearance of new lesions. In the present study, 21 of 24 HCCs were detected on the present non-enhanced, arterial-phase and the previous arterial-phase CT images, while 22 HCCs were detected using the additional

9

1   information from subtraction images. In addition, the dynamic and temporal subtraction images

2   increased the conspicuousness of HCC.

3   On objective evaluation of the quality of dynamic and temporal subtraction images, as the

4   levels of background noise of both subtraction images were higher than those of the present

5   arterial-phase CT images, SNR of both subtraction images were lower than those of the present

6   arterial-phase CT images. However, both subtraction images had uniform zero pixel values

7   except for regions with interval changes, *etc*. Therefore, nodule-to-liver contrast was higher in

8   both subtraction images than in present arterial-phase CT images.

9   In the present study, there was a difference in HCC classified as good in the dynamic and

10 temporal subtraction images. The difference was mainly due to misregistration of the hepatic

11 shape, which was related only to breath-holding on the dynamic subtraction images, while it

12 was related with breath-holding and hepatic deformity during the clinical course on temporal

13 subtraction images.

14   There have been a number of studies of computer-aided detection of HCC (Bellon *et al.*

15 1997, Voirin *et al.* 2002, Gletsos *et al.* 2003, Bilello *et al.* 2004). Gletsos *et al.* (2003) reported a

16 method for detecting and classifying HCC using texture analysis and an artificial neural network

17 (ANN) on non-enhanced CT images. Bilello *et al.* (2004) also reported a method for detecting

18 HCC on delayed-phase CT images. In their study, to achieve 90% sensitivity, the total

19 false-positive rate was increased to about 2.2 per section. In the present study, after assessing set

20 C (non-enhanced, arterial-phase and previous arterial-phase CT images), observers then

21 assessed both subtraction images. Therefore, there were no false-positives due to the enhanced

22 images. Screening for HCC by abdominal CT is widely performed in patients with liver

23 cirrhosis and hepatitis B and C. In general, there are no remarkable changes in liver shape

24 during such screening intervals, thus reducing the frequency of misregistration artefacts. It is

25 convenient to apply temporal subtraction for detection of HCC under such conditions. Therefore,

26 this technique using not only dynamic subtraction but also temporal subtraction may be

27 beneficial to radiologists for CT detection of HCC.

28

29   However, one nodule was not detected on both dynamic subtraction images using the

30 present CT images and temporal subtraction images. As shown in Figure 5, the radiologist could

1   not locate this tumour precisely on either image. In this case, different axial levels of the liver

2   were selected in the automated image-matching technique. Therefore, misregistration artefacts

3   appeared at the periphery of the liver. In addition, no definite staining characteristic of HCC was

4   observed, probably because of the relatively hypovascular nature of the lesion.

5   For good rating score, some misregistration artefacts appeared at the periphery of the liver

6   in dynamic subtraction images using the present CT images and temporal subtraction images

7   (Figs. 1–4). With regard to the manual global shift value, we obtained dynamic subtraction

8   images using the present CT images and temporal subtraction images in these cases, after

9   manual selection of image sets at the same anatomical positions from the present (non-enhanced

10   and contrast-enhanced images) and previous images. Less misregistration artefacts appeared at

11   the periphery of the liver in these images than in the automatic method.

12   The present study did not include cases with deformity of the liver due to treatment, such

13   as transcatheter arterial embolisation (TAE), percutaneous ethanol injection therapy (PEIT) or

14   radiofrequency ablation (RFA). In addition, changes in hepatic shape may be induced by local

15   atrophy of the liver between the present and previous images, ascites, or breath-holding.

16   Therefore, it may be difficult to select images from the same anatomical positions in such cases.

17   It is necessary to improve the precision of this automated image-matching technique for use in

18   such cases. Therefore, in future studies we intend to compare the volume data of the liver on

19   each of the previous and present images. Methods involving not only image shifting and

20   rotation techniques but also nonlinear geometric warping techniques for previous images (Kano

21   *et al.* 1993, Ishida *et al.* 1999) may improve the method developed here because of the

22   reduction of misregistration artefacts, especially on temporal subtraction images.

23   The results were obtained in a relatively small number of cases (14 cases) and with a

24   small number of observers (three observers). Therefore, to evaluate the clinical efficacy of this

25   technique, a prospective study (ROC type analysis) with larger numbers of patients is required.

26

27   **5. CONCLUSIONS**

28   We developed a computerised method for detecting moderately differentiated HCC using

29   dynamic and temporal subtraction images based on an automated image-matching technique.

30   This method may be useful for use of these subtraction images as reference images in detection

of small moderately differentiated HCC by CT.

7. REFERENCES

Abe H, Ishida T, Shiraishi J, Li F, Katsuragawa S, Sone S, MacMahon H and Doi K 2004 Effect of temporal subtraction images on Radiologists' detection of lung cancer on CT: result of the observer performance study with use of file computed tomography images *Acad Radiol.* **11** 1337-1343

Arimura H, Katsuragawa S, Li Q, Ishida T and Doi K 2002 Development of a computerized method for identifying the posteroanterior and lateral views of chest radiographs by use of a template matching technique *Med Phys.* **29(7)** 1556-1561

Baron R L and Peterson M S 2001 From the RSNA refresher courses: Screening the cirrhotic liver for hepatocellular carcinoma with CT and MR imaging *Radiographics.* **21** 117-132

Bellon E, Feron M, Maes F, Hoe L V, Delaere D, Haven F, Sunaert S, Baert A L, Marchal G and Suetens P 1997 Evaluation of manual vs semi-automated delineation of liver lesions on CT images *Eur Radiol.* **7(3)** 432-438

Bilello M, Gokturk S B, Desser T, Napel S, Jeffrey R B Jr and Beaulieu C F 2004 Automatic detection and classification of hypodense hepatic lesions on contrast-enhanced venous-phase CT *Med Phys.* **31(9)** 2584-2593

Biswas J, Nelson C B, Runge V M, Wintersperger B J, Baumann S S, Jackson C B, Dacvpm D D and Patel T 2005 Brain Tumor enhancement in magnetic resonance imaging comparison of signal-to-noise ratio (SNR) and contrast-to-noise ratio (CNR) at 1.5 versus 3 tesla *Invest Radiol.* **40** 792-797

Blachar A, Federle M P, Ferris J V, Lacomis J M, Waltz J S, Armfield D R, Chu G, Almusa O, Grazioli L, Balzano E and Li W 2002 Radiologists' Performance in the diagnosis of the liver tumor with central scars by using specific CT criteria *Radiology.* **223** 532-539

1   Ding H, Kudo M, Onda H, Suetomi Y, Minami Y and Maekawa K 2001 Contrast-enhanced
2   subtraction harmonicsonography for evaluating treatment response in patients with
3   hepatocellular carcinoma *AJR Am J Roentgenol.* **176(3)** 661-666

4   Farinati F and Gianni S 2001 Surveillance for hepatocellular carcinoma in cirrhosis: is it
5   cost-effective? *Eur J Cancer Prev.* **10(1)** 111-115

6   Gletsos M, Mougiakakou S G, Matsopoulos G K, Nikita K S, Nikita A S and Kelekis D 2003 A
7   computer-aided diagnostic system to characterize CT focal liver lesions: design and
8   optimization of a neural network classifier *IEEE Trans Inf Technol Biomed.* **7(3)** 153-162

9   Ishida T, Ashizawa K, Engelmann R, Katsuragawa S, MacMahon H and Doi K 1998
10   Application of temporal subtraction for detection of interval changes on chest
11   radiographs: improvement of subtraction images using automated initial image matching
12   *J.Dig. Imaging.* **12** 77-86

13   Ishida T, Katsuragawa S, Nakamura K, MacMahon H and Doi K 1999 Iterative image warping
14   technique for temporal subtraction of sequential chest radiographs to detect interval
15   change *Med Phys.* **26(7)** 1320-1329

16   Kano A, Doi K, MacMahon H, Hassell D D and Giger M L 1993 Digital image subtraction of
17   temporally sequential chest images for detection of interval change *Med Phys.* **21(3)**
18   453-461

19   Kim C K, Lim J H and Lee W J 2001 Detection of hepatocellular carcinomas and dysplastic
20   nodules in cirrhotic liver: accuracy of ultrasonography in transplant patients *J Ultrasound*
21   *Med.* **20(2)** 99-104

22   Morishita J, Katsuragawa S, Kondo K and Dio K 2001 An automated patient recognition
23   method based on an image-matching technique using previous chest radiographs in the
24   picture archiving and communication system environment *Med Phys.* **28(6)** 1093-1097

25   Morishita J, Katsuragawa S, Sasaki Y and Doi K 2004 Potential usefulness of biological
26   fingerprints in chest radiographs for automated patient recognition and identification *Acad*
27   *Radiol.* **11** 309-315

28   Okumura E, Sanada S, Suzuki M, Tsushima Y and Matsui O 2005 Automated Image-matching
29   Technique for Comparative Diagnosis of the Liver on CT Examination Nippon Hoshasen
30   Gijutsu Gakkai Zasshi. **61(12)** 1616-22.

Peterson MS, Baron R L, Marsh J W Jr, Oliver J H 3rd, Confer S R and Hunt L E 2000
Pretransplantation surveillance for possible hepatocellular carcinoma in patients with
cirrhosis: epidemiology and CT-based tumor detection rate in 430 cases with surgical
pathologic correlation *Radiology.* **217** 743-749

Soyer P, Spelle L, Gouhiri M H, Rondeau Y, Pelage J P, Scherrer A and Rymer R 1999
Gadolinium chelate-enhanced subtraction spoiled gradient-recalled echo MR imaging of
hepatic tumors *AJR Am J Roentgenol.* **172(1)** 79-82

Spielmann A L, Nelson R C, Lowry C R, Johnson G A, Sundaramoothy G, Sheafor D H and
Paulson E K 2002 Liver: single breath-hold dynamic subtraction CT with multi-detector
row helical technology feasibility study *Radiology.* **222(1)** 278-283

Voirin D, Payan Y, Amavizca M, Letoublon C and Troccaz J 2002 Computer-aided hepatic
tumour ablation: requirements and preliminary results *C R Biol.* **325(4)** 309-319

Yu J S and Rofsky N M 2003 Dynamic subtraction MR imaging of the liver: advantages and
pitfalls *AJR Am J Roentgenol.* **180(5)** 1351-1357

Ward J and Robinson P J 2002 How to detect hepatocellular carcinoma in cirrhosis *Eur Radiol.*
12 2258-2272

Figure 1. A 76-year-old woman with moderately differentiated HCC ($S_{4/8}$). (a) Present non-enhanced CT. An area of low density was seen in $S_{4/8}$. (b) Present arterial-phase CT. Nodular early enhancement was seen (black arrow). (c) Previous arterial-phase CT. No definite abnormal enhancement was observed. (d) Late-phase CTHA was performed following the present CT, and ring enhancement was seen. The lesion was diagnosed as moderately differentiated HCC. (e) Dynamic subtraction image using the present CT image. HCC was observed more clearly as nodular enhancement (white arrow). (f) Temporal subtraction image. Nodular enhancement was observed, and HCC was a new lesion that appeared during the follow-up period.

Figure 2. A 76-year-old woman with moderately differentiated HCC ($S_{2/3}$) (the same patient as in Fig. 1). (a) Present non-enhanced CT. No definite low-density area was seen in $S_{2/3}$. (b) Present arterial-phase CT. Nodular enhancement was seen (black arrow). (c) Previous

arterial-phase CT. A minute area of nodular early enhancement was seen, but was suspected to be a small A-P shunt. (d) CTAP was performed following the present CT. A round defect of portal flow was observed. The lesion was diagnosed as HCC. (e) Dynamic subtraction image using the present CT image. The nodular enhancement was observed more clearly in $S_{2/3}$ (white arrow). (f) Temporal subtraction image. Ring enhancement was observed and the lesion increased in size during the follow-up period.

Figure 3. A 76-year-old woman with moderately differentiated HCC (S_5) (the same patient as in Fig. 1). (a) Present non-enhanced CT. No definite lesions were observed. (b) Present arterial-phase CT. A small area of nodular early enhancement was suspected (black arrow). (c) Previous arterial-phase CT. No definite abnormal enhancement was observed. (d) CTAP was performed following the present CT. A round defect of portal flow was observed. The lesion was diagnosed as HCC. (e) Dynamic subtraction image using the present CT image. The nodular enhancement was seen more clearly (white arrow). (f) Temporal subtraction image. Nodular enhancement was observed, and HCC was a new lesion that appeared during the follow-up period.

Figure 4. A 61-year-old man with moderately differentiated HCC (S_8). (a) Present non-enhanced CT. No definite lesion was found. (b) Present arterial-phase CT. Nodular early enhancement was observed (black arrow). (c) Previous arterial-phase CT. A small area of nodular early enhancement was observed. (d) The early phase of CTHA was performed following the present CT. Nodular enhancement was observed in S_8. The lesion was diagnosed as HCC. (e) Dynamic subtraction image using the present CT image. The nodular enhancement was seen more clearly (white arrow). (f) Temporal subtraction image. Ring enhancement was observed and the lesion increased in size during the follow-up period.

Figure 5. A 74-year-old man with moderately differentiated HCC (S_7). (a) Present non-enhanced CT. An area of low density was seen. (b) Present arterial-phase CT. An area of low density was seen (black arrow). (c) Previous arterial-phase CT. No definite abnormal enhancement was observed. (d) CTAP was performed following the present CT. A round defect of portal flow was

observed. The lesion was diagnosed as HCC. (e) Dynamic subtraction image using the present CT image. No definite nodular staining was observed expect for vague peripheral enhancement (white arrow). (f) Temporal subtraction image. No definite nodular staining was observed. A misregistration artefact was seen, as shown in (e) and (f).

Table 1. Comparison of average values and SD of nodule-to-liver contrast and SNR of the present arterial-phase CT images and (a) dynamic subtraction images using the present CT images and (b) temporal subtraction images.
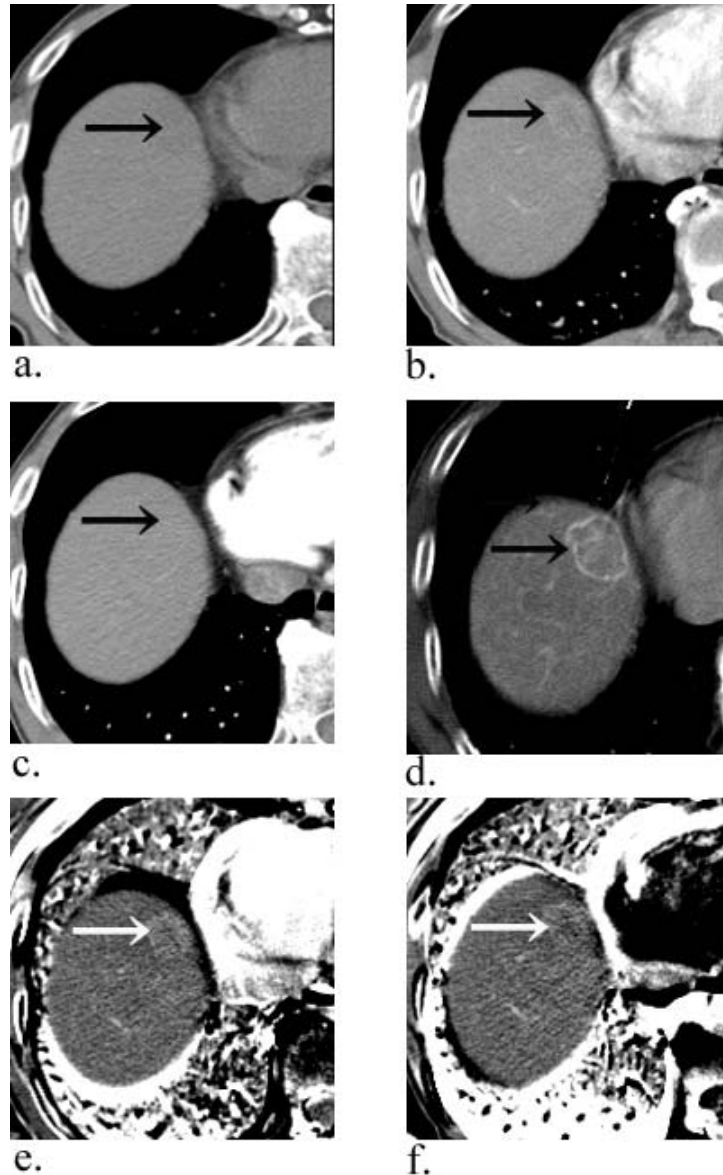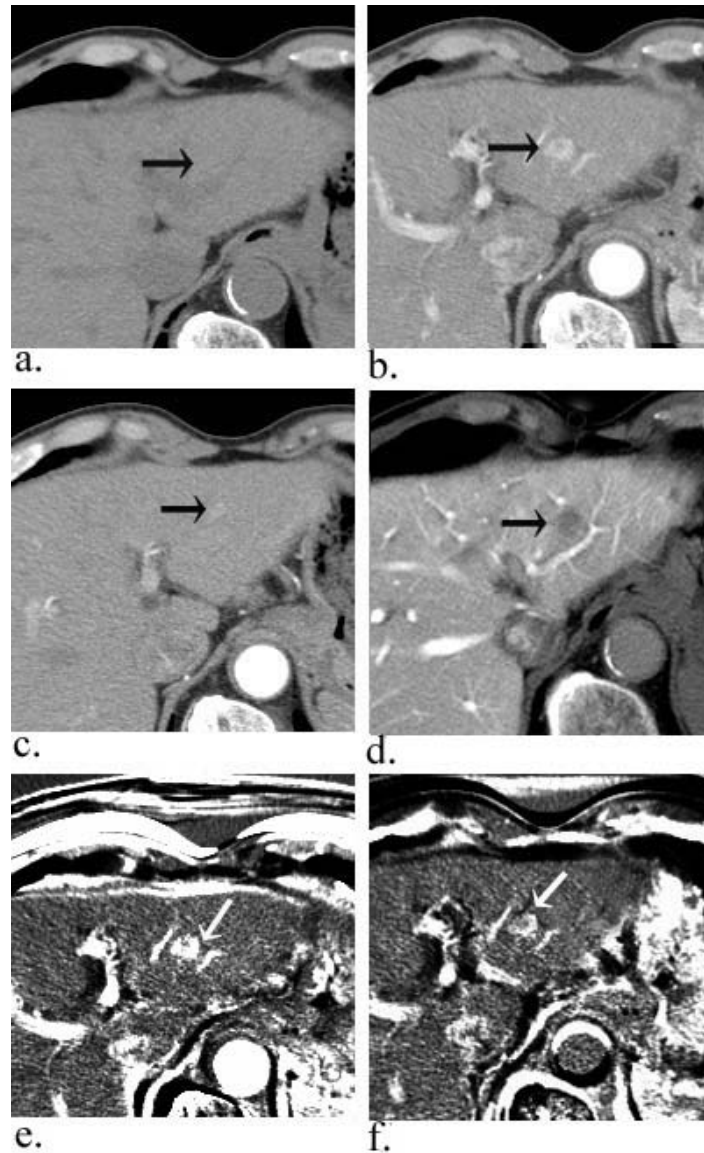
1

2   Figure 1. A 76-year-old woman with moderately differentiated HCC ($S_{4/8}$). (a) Present

3   non-enhanced CT. An area of low density was seen in $S_{4/8}$. (b) Present arterial-phase CT.

4   Nodular early enhancement was seen (black arrow). (c) Previous arterial-phase CT. No definite

5   abnormal enhancement was observed. (d) Late-phase CTHA was performed following the

6   present CT, and ring enhancement was seen. The lesion was diagnosed as moderately

7   differentiated HCC. (e) Dynamic subtraction image using the present CT image. HCC was

8   observed more clearly as nodular enhancement (white arrow). (f) Temporal subtraction image.

9   Nodular enhancement was observed, and HCC was a new lesion that appeared during the
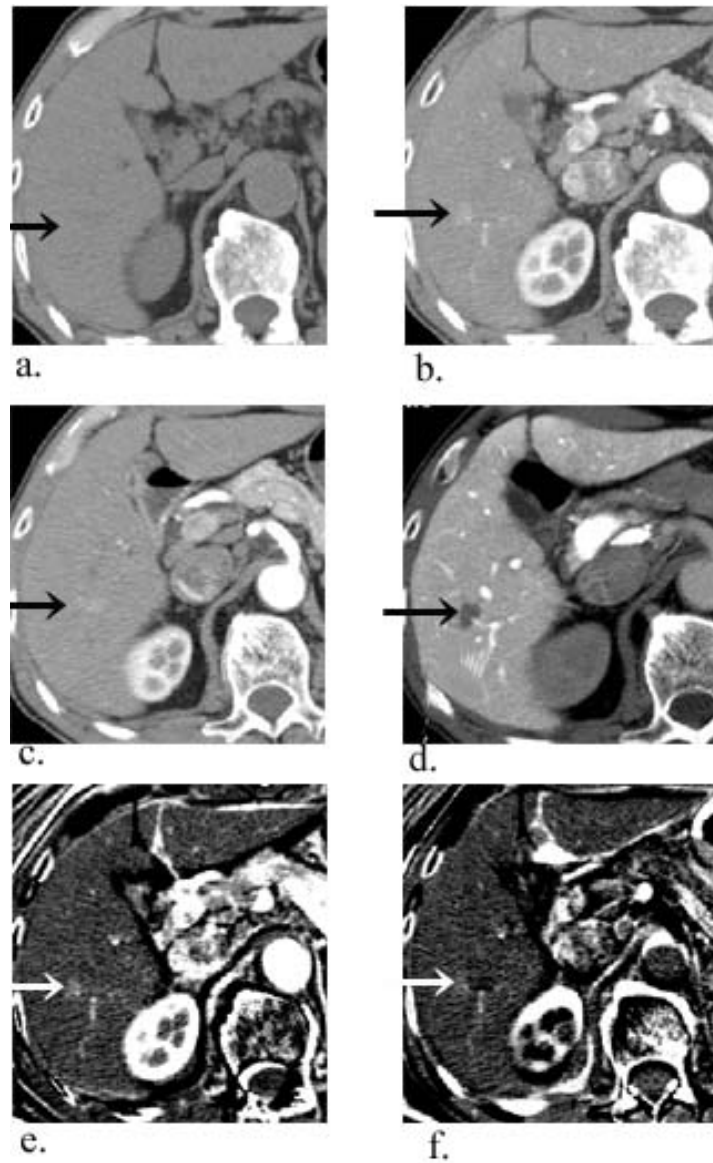
10   follow-up period.

1

2

3   Figure 2. A 76-year-old woman with moderately differentiated HCC ($S_{2/3}$) (the same patient as

4   in Fig. 1). (a) Present non-enhanced CT. No definite low-density area was seen in $S_{2/3}$. (b)

5   Present arterial-phase CT. Nodular enhancement was seen (black arrow). (c) Previous

6   arterial-phase CT. A minute area of nodular early enhancement was seen, but was suspected to

7   be a small A-P shunt. (d) CTAP was performed following the present CT. A round defect of

8   portal flow was observed. The lesion was diagnosed as HCC. (e) Dynamic subtraction image

9   using the present CT image. The nodular enhancement was observed more clearly in $S_{2/3}$ (white

10   arrow). (f) Temporal subtraction image. Ring enhancement was observed and the lesion

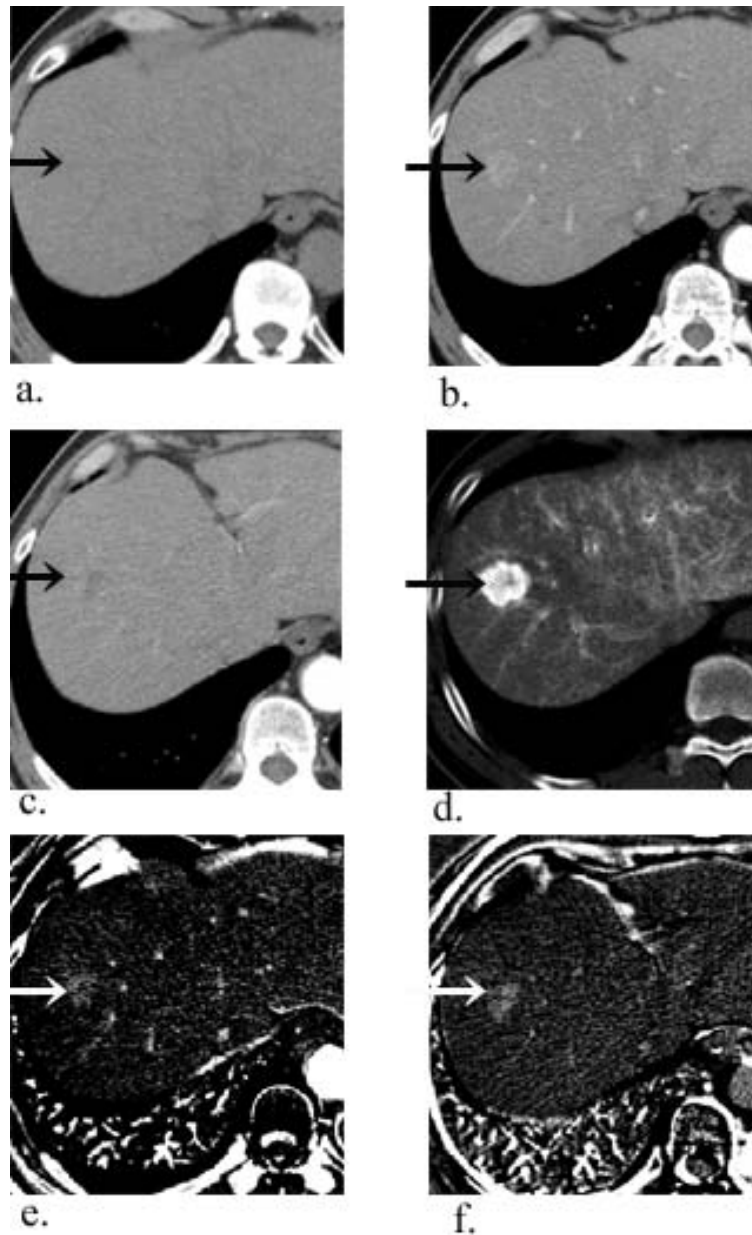11   increased in size during the follow-up period.

1

2

Figure 3. A 76-year-old woman with moderately differentiated HCC (S_5) (the same patient as in Fig. 1). (a) Present non-enhanced CT. No definite lesions were observed. (b) Present arterial-phase CT. A small area of nodular early enhancement was suspected (black arrow). (c) Previous arterial-phase CT. No definite abnormal enhancement was observed. (d) CTAP was performed following the present CT. A round defect of portal flow was observed. The lesion was diagnosed as HCC. (e) Dynamic subtraction image using the present CT image. The nodular enhancement was seen more clearly (white arrow). (f) Temporal subtraction image. Nodular enhancement was observed, and HCC was a new lesion that appeared during the follow-up
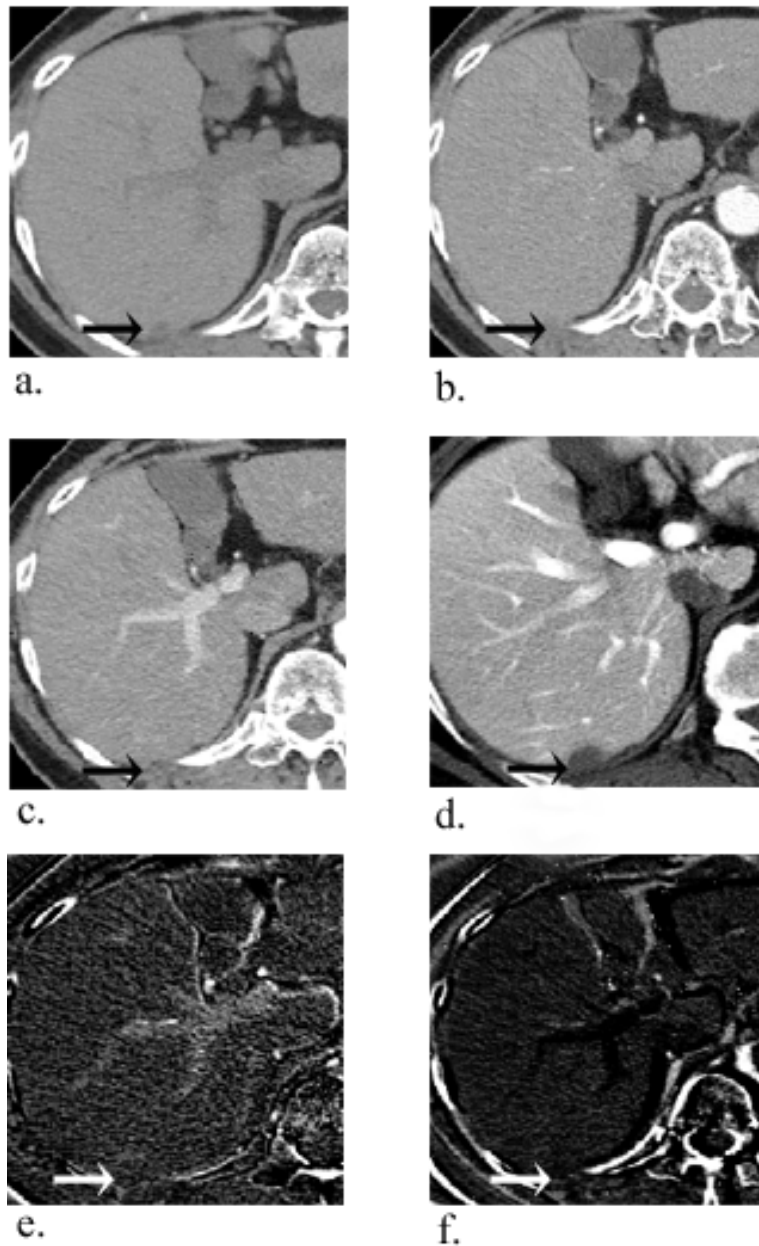
1   period.

2

3   Figure 4. A 61-year-old man with moderately differentiated HCC (S_8). (a) Present non-enhanced

4   CT. No definite lesion was found. (b) Present arterial-phase CT. Nodular early enhancement was

5   observed (black arrow). (c) Previous arterial-phase CT. A small area of nodular early

6   enhancement was observed. (d) The early phase of CTHA was performed following the present

7   CT. Nodular enhancement was observed in S_8. The lesion was diagnosed as HCC. (e) Dynamic

8   subtraction image using the present CT image. The nodular enhancement was seen more clearly

9   (white arrow). (f) Temporal subtraction image. Ring enhancement was observed and the lesion

1 increased in size during the follow-up period.

2

3 Figure 5. A 74-year-old man with moderately differentiated HCC (S$_7$). (a) Present non-enhanced

4 CT. An area of low density was seen. (b) Present arterial-phase CT. An area of low density was

5 seen (black arrow). (c) Previous arterial-phase CT. No definite abnormal enhancement was

6 observed. (d) CTAP was performed following the present CT. A round defect of portal flow was

7 observed. The lesion was diagnosed as HCC. (e) Dynamic subtraction image using the present

8 CT image. No definite nodular staining was observed expect for vague peripheral enhancement

9 (white arrow). (f) Temporal subtraction image. No definite nodular staining was observed. A

1 misregistration artefact was seen, as shown in (e) and (f).

2 Table 1. Comparison of average values and SD of nodule-to-liver contrast and SNR of the

3 present arterial-phase CT images and (a) dynamic subtraction images using the present CT

4 images and (b) temporal subtraction images.

	Present arterial-phase CT images (A)	Dynamic subtraction images (B)	(B/A)×100 [%]	P
Nodule-to-liver contrast	29.5±12.7	39.0±14.0	150	0.0001
Liver of SNR	16.2±7.8	2.2±1.4	13	0.000008
Nodule of SNR	22.5±7.8	8.2±3.0	40	0.0001

(a)

	Present arterial-phase CT images (A)	Temporal subtraction images (B)	(B/A)×100 [%]	P
Nodule-to-liver contrast	28.7±12.4	38.0±16.0	140	0.0004
Liver of SNR	14.7±3.5	0.1±0.6	10	0.0004
Nodule of SNR	20.4±5.7	8.0±10.0	34	0.0004

5 (b)